Langmuir
Article
pubs.acs.org/Langmuir

Adhesion of Nanoparticles

Jan-Michael Y. Carrillo,[†] Elie Raphael,[‡] and Andrey V. Dobrynin*,[†]

[†]*Polymer Program, Institute of Materials Science, and Department of Physics, University of Connecticut, Storrs, Connecticut 06268, and* [‡]*PCT Lab., UMR CNRS Gulliver 7083, ESPCI, 10 rue Vauquelin, 75231 Paris Cedex 05, France*

Received May 17, 2010. Revised Manuscript Received June 17, 2010

We have developed a new model of nanoparticle adhesion which explicitly takes into account the change in the nanoparticle surface energy. Using combination of the molecular dynamics simulations and theoretical calculations we have showed that the deformation of the adsorbed nanoparticles is a function of the dimensionless parameter $\beta \propto \gamma_p(GR_p)^{-2/3}W^{-1/3}$, where G is the particle shear modulus, R_p is the initial particle radius, γ_p is the polymer interfacial energy, and W is the particle work of adhesion. In the case of small values of the parameter $\beta < 0.1$, which is usually the case for strongly cross-linked large nanoparticles, the particle deformation can be described in the framework of the classical Johnson, Kendall, and Roberts (JKR) theory. However, we observed a significant deviation from the classical JKR theory in the case of the weakly cross-linked nanoparticles that experience large shape deformations upon particle adhesion. In this case the interfacial energy of the nanoparticle plays an important role controlling nanoparticle deformation. Our model of the nanoparticle adhesion is in a very good agreement with the simulation results and provides a new universal scaling relationship for nanoparticle deformation as a function of the system parameters.

Adhesion phenomena play an important role in different areas of science and technology including tribology,[1−3] colloidal science,[4,5] materials science,[6−10] biophysics, and biochemistry.[11−13] They are of paramount importance for colloidal stabilization, drug delivery, interfacial friction and lubrication, nanofabrication and nanomolding, cell mechanics and adhesion, and contact mechanics. The modern approach to adhesion between elastic bodies in a contact is based on the classical work by Johnson, Kendal and Roberts (JKR)[14] that extended the Hertz theory[15] of the elastic contact by accounting for the effect of the adhesion in the contact area. According to this model a contact radius a of an elastic sphere of radius R_p with the shear modulus G in a contact with a solid substrate is proportional to $a \propto R_p(W/GR_p)^{1/3}$, where W is the work of adhesion (for reviews see refs 2, 7, and 15). The analysis of this scaling relation indicates that the importance of the adhesive forces increases for "soft" highly compliant materials such as elastomers, living cells and soft tissues.

However, the JKR theory[14,15] only takes into account the change in the particle surface energy in the contact area with the substrate and completely ignores contribution from the change in the surface energy of a particle due to its shape deformation. This effect is small for the large particles for which the work of adhesion W is smaller than GR_p. Unfortunately when the opposite inequality holds, $W > GR_p$, a particle undergoes large deformations with the contact radius being on the order of the initial particle size. For example, a latex particle with a shear modulus $G \approx 10^6$ Pa adsorbed on a silicon wafer surface with the work of adhesion $W \approx 100$ mJ/m^2 will undergo significant deformation when its size is smaller than $W/G \approx 100$. Thus, for nanoparticles the elastic energy of particle deformation GR_p^3 becomes comparable with its surface energy $\gamma_p R_p^2 \approx WR_p^2$ which has to be taken into account in calculating the equilibrium particle shape. In this paper we will consider adhesion of a soft nanoparticle on a rigid substrate and will develop a general approach to describe nanoparticle deformation which in addition to the JKR model takes into account the change in the nanoparticle surface energy outside the contact area.

The total free energy of the deformed nanoparticle includes nanoparticle surface energy, van der Waals energy[5] of interaction of the nanoparticle with a substrate and the elastic energy contribution due to particle deformation. The particle deformation can be described by approximating a deformed nanoparticle by a spherical cap with radius R_1 and height h (see Figure 1). In addition we have also assumed that deformation of the nanoparticle occurs at a constant volume. This constraint allowed us to relate the radius of the deformed nanoparticle R_1 with the nanoparticle height h and initial nanoparticle size R_p. In the framework of this approximation one can calculate the nanoparticle free energy as a function of the nanoparticle deformation $1-h/2R_p = \Delta h/2R_p$. The details of calculations are given in the Appendix A.

In the case of small deformations $\Delta h/R_p \ll 1$ the nanoparticle free energy has a simple analytical form

$$F(\Delta h) \propto -2\pi WR_p\Delta h + \pi\gamma_p\Delta h^2 + \frac{7\sqrt{2}}{15}KR_p^{1/2}\Delta h^{5/2} \qquad (1)$$

The first term in the r.h.s of the eq 1 represents contribution of the long-range van der Waals interactions of the deformed nanoparticle with a substrate where W is the work of adhesion. The second

*To whom correspondence should be addressed.

(1) Crosby, A. J.; Shull, K. R. *J. Polym. Sci., Part B: Polym. Phys.* **1999**, *37*(24), 3455–3472.
(2) Johnson, K. L. *Tribol. Int.l* **1998**, *31*(8), 413–418.
(3) Mo, Y. F.; Turner, K. T.; Szlufarska, I. *Nature* **2009**, *457*(7233), 1116–1119.
(4) de Gennes, P.-G.; Brochard-Wyart, F.; Quere, D. *Capillarity and Wetting Phenomena*; Springer: New York, 2002.
(5) Israelachvili, J. *Intermolecular and Surface Forces*; Academic Press: London, 1992.
(6) Gerberich, W. W.; Cordill, M. J. *Rep. Prog. Phys.* **2006**, *69*(7), 2157–2203.
(7) Barthel, E. *J. Phys. D: Appl. Phys.* **2008**, *41*, 163001.
(8) Luan, B. Q.; Robbins, M. O. *Nature* **2005**, *435*(7044), 929–932.
(9) Shull, K. R. *Mater. Sci. Eng. R-Rep.* **2002**, *36*(1), 1–45.
(10) Shull, K. R.; Creton, C. *J. Polym. Sci., Part B: Polym. Phys.* **2004**, *42*(22), 4023–4043.
(11) Arzt, E.; Gorb, S.; Spolenak, R. *Proc. Natl. Acad. Sci. U.S.A.* **2003**, *100*(19), 10603–10606.
(12) Lin, D. C.; Horkay, F. *Soft Matter* **2008**, *4*(4), 669–682.
(13) Liu, K. K. *J. Phys. D: Appl. Phys.* **2006**, *39*(11), R189–R199.
(14) Johnson, K. L.; Kendall, K.; Roberts, A. D. *Proc. R. Soc. London A* **1971**, *324*, 301–313.
(15) Johnson, K. L. *Contact Mechanics*, 9th ed.; Cambridge University Press: New York, 2003.

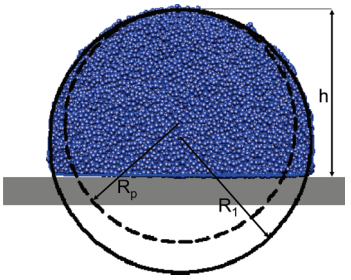

Figure 1. Snapshot of the deformed nanoparticle and schematic representation of approximation of its shape by a spherical cap with radius R_1 (solid line). The shape of the undeformed nanoparticle with radius R_p is shown by a dashed line.

term describes the increase of the surface energy of the spherical cap (deformed nanoparticle) with the interfacial energy γ_p in comparison with that of a sphere with radius R_p. Finally, the last term is the elastic energy contribution[16] due to deformation of a nanoparticle with rigidity $K = 2G/(1-\nu)$, where G is the particle shear modulus and ν is the Poisson ratio. Note, that for deformation at a constant volume $\nu = 0.5$ which results in $K = 4G$.

The equilibrium deformation of the adsorbed nanoparticle is obtained by minimizing nanoparticle free energy eq 1 with respect to Δh. This results in the following equation for the nanoparticle deformation

$$0 = -2\pi W R_p + 2\pi\gamma_p \Delta h + \frac{7\sqrt{2}}{6} K R_p^{1/2} \Delta h^{3/2} \qquad (2)$$

Introducing dimensionless variables $y^2 = \frac{\Delta h}{2R_p A}\left(\frac{KR_p}{W}\right)^{2/3}$ and $\beta = B\left(\frac{\gamma_p^{3/2}}{KR_p W^{1/2}}\right)^{2/3}$ (where $A = (3\pi/7)^{2/3}$ and $B = 2(3\pi/7)^{2/3}$ are numerical coefficients) we can reduce eq 2 to a simple cubic equation

$$0 = -1 + \beta y^2 + y^3 \qquad (3)$$

The deformation of the nanoparticle is described by a positive root of this equation

$$\frac{\Delta h}{2R_p} = A\left(\frac{W}{KR_p}\right)^{2/3}\left(\sqrt[3]{r+\sqrt{q^3+r^2}} + \sqrt[3]{r-\sqrt{q^3+r^2}} - \frac{\beta}{3}\right)^2 \qquad (4)$$

where

$$r = \frac{1}{2} - \left(\frac{\beta}{3}\right)^3, \quad \text{and} \quad q = -\left(\frac{\beta}{3}\right)^2 \qquad (5)$$

Note, that the values of the numerical coefficients in the eq 4, $A = (3\pi/7)^{2/3}$ and $B = 2A = 2(3\pi/7)^{2/3}$, depend on the particular nanoparticle shape and deformation that was used for calculation of the different terms in the nanoparticle free energy (see Appendix A). Thus, we expect the values of these coefficients to be model dependent. However, we do not expect the form of the equation and scaling relations to change. One can also express reduced parameters in terms of the shear modulus G. In this case the values of the numerical coefficients are $A_G = A((1-\nu)/2)^{2/3} = (3\pi(1-\nu)/14)^{2/3}$ and $B_G = 2A_G$.

The analysis of eq 3 points out that the dimensionless parameter β determines the relative strength of the interfacial and elastic energy contributions. For small values of the parameter $\beta \approx \gamma_p (KR_p)^{-2/3} W^{-1/3} \ll 1$ the equilibrium nanoparticle height is determined by balancing the first and the last terms in the rhs of the equation eq 3. In this case the penalty for the elastic deformation of the nanoparticle stabilizes its height. This corresponds to the JKR-scaling[14] dependence of the nanoparticle deformation $\Delta h \propto R_p (W/KR_p)^{2/3}$. This is usually the case for large strongly cross-linked nanoparticles. In the opposite limit of large values of the parameter β (small weakly cross-linked nanoparticles), the deformation of the nanoparticle height is proportional to the ratio of the interfacial and surface energies $\Delta h \propto R_p W/\gamma_p$. This corresponds to the droplet wetting regime when interfacial and surface energies determine the equilibrium droplet shape at the substrate.[4]

To test our model we have performed molecular dynamics simulations[17] of the adhesion of spherical polymeric nanoparticles on a solid substrate. In our simulations nanoparticles were made of cross-linked linear chains. We used a coarse-grained representation of polymer chains. In this representation monomers were modeled by the Lennard-Jones particles with diameter σ. The connectivity of monomers into polymer chains was maintained by the FENE potential. The same bond potential was used to model cross-links between polymer chains forming a nanoparticle. We set the value of the Lennard-Jones interaction parameter for the polymer−polymer pair to $\varepsilon_{LJ} = 1.5 k_B T$ (where k_B is the Boltzmann constant and T is the absolute temperature) which corresponds to a poor solvent conditions for the polymer backbone. The elastic properties of the nanoparticles were varied by changing the density of the cross-links between linear chains forming a nanoparticle. The values of the shear modulus G for the nanoparticles with different cross-linking densities ρ_c were obtained by performing simulations of deformation of the 3-D networks with the same polymer density and number density of the cross-links.[18] The interaction of a solid substrate with monomers forming a nanoparticle was modeled by the 3−9 potential with the value of the interaction parameter ε_w. We performed simulations with $\varepsilon_w = 1.5 k_B T$, $2.25 k_B T$ and $3.0 k_B T$. The explicit form of the interaction potentials, bond potential, and simulation details are given in the Appendix B.

Figure 2 shows dependence of the nanoparticle shape on the strength of the long-range van der Waals interactions with the substrate and the particle shear modulus, G. For the strongly cross-linked nanoparticles corresponding to the large values of the shear modulus G the increase in strength of the substrate-nanoparticle interactions leads only to small particle deformations. For this range of the interaction parameters and nanoparticle shear modulus the value of the contact angle $\theta > 90°$. The elasticity of the nanoparticle leads to the effective surface-phobic interactions of a nanoparticle with a substrate. The value of the contact angle decreases with increasing the strength of the substrate−nanoparticle interactions and decreasing the value of the shear modulus. Decrease in the nanoparticle shear modulus lowers the elastic energy penalty for particle deformation allowing large particle shape deformations at the same strength of the substrate−nanoparticle interactions. Weakly cross-linked nanoparticles show high affinity to the substrate which is manifested in smaller values of the contact angle. In some cases the value of the contact angle could be $\theta < 90°$. Note, that the changes in the particle contact angle are coupled with changes in the nanoparticle height and particle contact radius with the substrate. Thus, there exists a peculiar interplay of the interfacial and elastic energies in determining the equilibrium shape of a nanoparticle.

(16) Lau, A. W. C.; Portigliatti, M.; Raphael, E.; Leger, L. *Europhys. Lett.* **2002**, *60*(5), 717–723.

(17) Frenkel, D.; Smit, B. *Understanding Molecular Simulations*; Academic Press: New York, 2002.

(18) Carrillo, J. M. Y.; Dobrynin, A. V. *Langmuir* **2009**, *25*(22), 13244–13249.

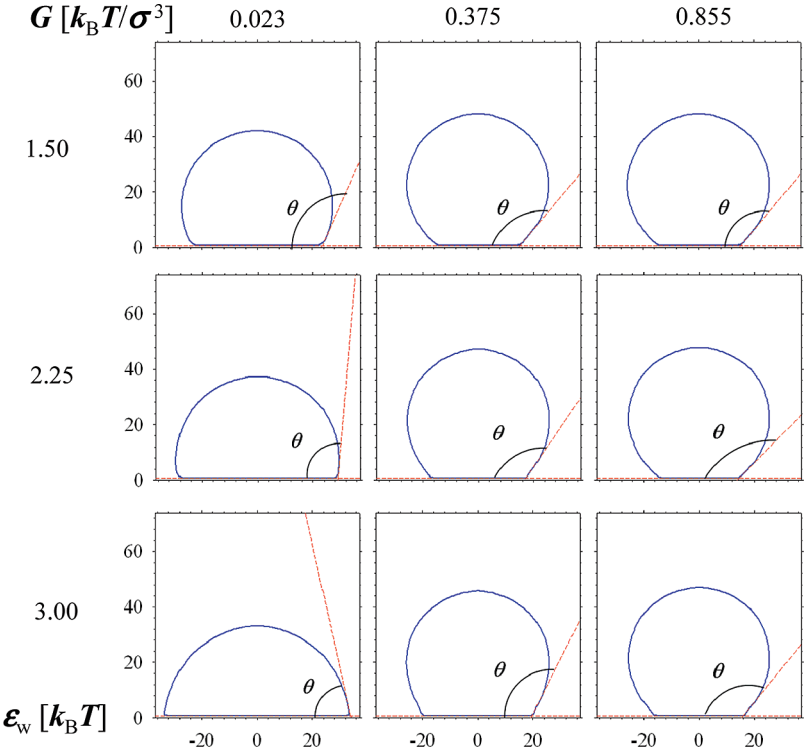

Figure 2. Dependence of the average shape of a nanoparticle and a contact angle on the value of the nanoparticle shear modulus G and the strength of the nanoparticle substrate interaction potential ε_w.

Figure 3 shows dependence of the reduced particle deformation $(GR_p/W)^{2/3}\Delta h/2R_p$ on the value of the parameter $\gamma_p(GR_p)^{-2/3}W^{-1/3}$. For this plot the values of the nanoparticle surface energy γ_p were obtained by performing simulations of the polymeric networks with the same value of the cross-linking density, LJ-interaction parameter $\varepsilon_{LJ} = 1.5k_BT$, and average density as those for nanoparticles (see Appendix B). The value of the parameter $d_0 = 0.867\sigma$ and average monomer density ρ_p used for calculations of the work of adhesion $W = \varepsilon_w\rho_p\sigma^3 d_0^{-2}/2$ (see eq A.6) were obtained from simulations. The solid line in Figure 3 is the best fit to the eq 4. The agreement between simulation results and theory is a very good. Thus, our simple scaling model correctly accounts for the effect of particle adhesion, surface energy and energy of the elastic deformation in determining the equilibrium particle shape. Note, that the numerical coefficients obtained from the fitting procedure are different from the numerical coefficients in the eq 4. This should not be surprising since we used an approximated expression for the elastic energy of the nanoparticle deformation (see Appendix A) which can explain this discrepancy. Using our simulation results we can set numerical coefficients in the eq 4 to be equal to $A_G = 0.419$ and $B_G = 0.28$ and consider this equation as an interpolation formula describing a crossover from JKR to nanoparticle wetting regime. This equation can be used to estimate the adhesion energy by studying the adhesion of nanoparticles of different sizes by fitting the experimental data for nanoparticle deformation to the eq 4 and considering dimensionless parameters $\gamma_p(GR_p)^{-2/3}W^{-1/3}$ and $(GR_p/W)^{2/3}$ as adjustable parameters. In addition one can also establish the boundary of the JKR regime[14] where the elastic energy plays the dominant role in controlling nanoparticle deformation. The dashed-line in Figure 3 corresponds to the JKR-like nanoparticle deformation. It follows from this figure that a crossover to the JKR regime can be estimated to occur at $\gamma_p \approx 0.1(GR_p)^{2/3}W^{1/3}$. Thus, knowing the material properties one can estimate for what nanoparticle sizes the deformation of a nanoparticle at a substrate

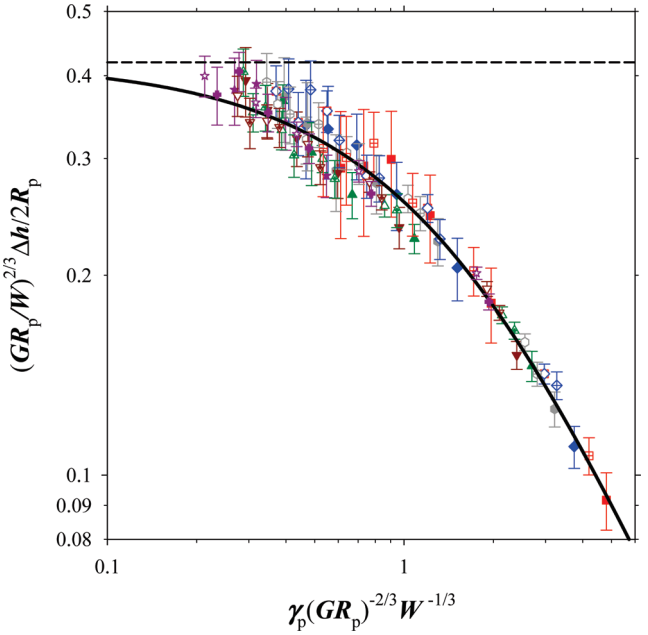

Figure 3. Dependence of the reduced nanoparticle deformation on the value of the parameter $\gamma_p(GR_p)^{-2/3}W^{-1/3}$ for nanoparticles with different cross-linking densities, different strengths of the substrate−polymer interaction parameter $\varepsilon_w = 1.5k_BT$ (filled symbols), $2.25k_BT$ (crossed symbols), $3.0k_BT$ (open symbols) and different nanoparticle sizes: $R_0 = 11.3\sigma$ (squares), 16.4σ (rhombs), 20.5σ (hexagons), 26.7σ (triangles), 31.8σ (inverted triangles), and 36.0σ (stars). (R_0 is the size of the cavity in which a nanoparticle was prepared (see Appendix B for details).) The solid line is the best fit to the eq 4 by considering numerical coefficients as fitting parameters $A_G = 0.419$, $B_G = 0.28$. For this fit we set $K = 4G$ because deformation of a nanoparticle occurs at almost constant volume (the Poisson ratio $\nu \approx 0.5$). The dashed line corresponds to JKR limit of nanoparticle deformation.

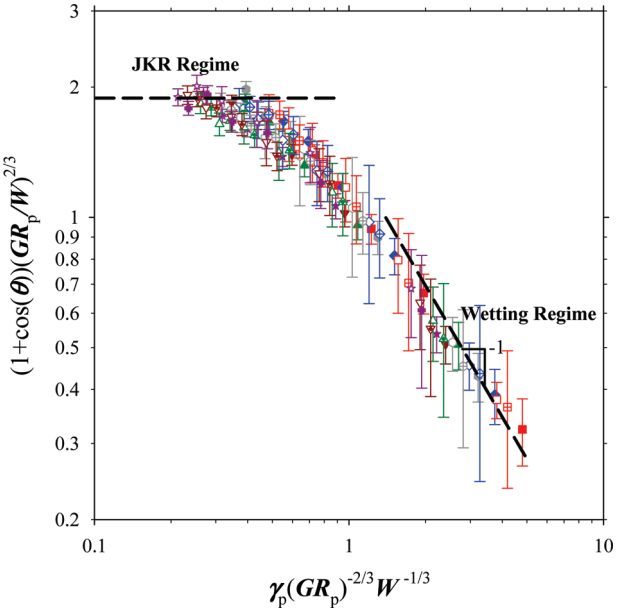

Figure 4. Dependence of the reduced value of the cosine of the nanoparticle contact angle on the value of the parameter $\gamma_p(GR_p)^{-2/3}W^{-1/3}$ for nanoparticles with different cross-linking densities, different strengths of the substrate−polymer interaction parameter ε_w and different nanoparticle sizes. Notations are the same as in Figure 3. The dashed lines show two different asymptotic regimes.

will be controlled by the nanoparticle surface energy, $R_p < 10^{3/2}\gamma_p{}^{3/2}/W^{1/2}G$.

One can also derive a scaling relation for the nanoparticle contact angle. For small deformations the nanoparticle contact angle can be approximated as

$$\cos(\theta) \approx -1+\frac{\Delta h}{R_p} \tag{6}$$

It is interesting to point out, that in the case when the nanoparticle shear modulus approaches zero, $G \to 0$, solution of the eq 2 reduces to $\Delta h/R_p \approx W/\gamma_p$ and eq 6 reproduces the Young-Dupre equation,[4] $W \approx \gamma_p(1+\cos(\theta))$. In Figure 4 we used reduced variables to collapse our simulation data into one universal plot. While the collapse of the data is good there is a difference by a factor of 2 from the value of $(GR_p/W)^{2/3}(1+\cos(\theta))$ expected from eq 6 and from the plot in Figure 3 for the same values of the parameter $\gamma_p(GR_p)^{-2/3}W^{-1/3}$. This tells us that the actual value of the contact angle is different from the macroscopic value which is obtained by fitting the nanoparticle shape by a spherical cap. This indicates that local forces acting on the contact line control the value of the contact angle. One can identify two different scaling regimes in Figure 4. In the range of small values of the parameter $\gamma_p(GR_p)^{-2/3}W^{-1/3} < 1$, we see a saturation of the value of $(GR_p/W)^{2/3}(1+\cos(\theta))$ which corresponds to the crossover to the JKR regime with $\Delta h/R_p \approx (W/GR_p)^{2/3}$. However, with increasing the value of the parameter $\gamma_p(GR_p)^{-2/3}W^{-1/3}$ the data points approach a line with slope −1. This represents a crossover to the nanoparticle wetting regime where the value of the contact angle is given by the Young−Dupre equation.[4]

We presented results of the molecular dynamics simulations and analytical calculations and showed that adhesion of a nanoparticle to a substrate is a result of the fine interplay between particle elastic, interfacial and adhesion energies. Depending on the value of the dimensionless parameter $\gamma_p(GR_p)^{-2/3}W^{-1/3}$ a nanoparticle deformation can be described either by balancing the particle elastic energy with a particle adhesion energy (the JKR regime $\gamma_p(GR_p)^{-2/3}W^{-1/3} \ll 1$) or by balancing the nanoparticle adhesion energy and interfacial energy (the nanoparticle wetting regime $\gamma_p(GR_p)^{-2/3}W^{-1/3} \gg 1$). We expect that a new mechanism for particle adhesion will play an important role in understanding contact mechanics of nanoscale objects, stability of soft nanoparticle in solutions, and friction and lubrication of nanostructured surfaces.

Acknowledgment. This work was supported by the Donors of the American Chemical Society Petroleum Research Fund under the Grant PRF # 49866-ND7.

Appendix A: Model of Nanoparticle Adhesion

The equilibrium shape of the particle is a result of optimization of the nanoparticle surface energy, its interaction with the substrate, and the elastic energy due to deformation of the particle shape. To evaluate different contributions to the nanoparticle free energy we assume that deformation of the adsorbed nanoparticle occurs at a constant volume and the deformed particle has shape of a spherical cap with radius R_1 and height h (see Figure 1).

$$R_1 = \frac{4R_p{}^3}{3h^2}+\frac{h}{3} \tag{A.1}$$

The surface energy of the spherical cap with interfacial energy γ_p is equal to

$$U_s(h) = \gamma_p(\pi a^2+2\pi R_1 h) = \pi\gamma_p(4R_1 h-h^2) \tag{A.2}$$

where the surface energy include contribution from the nanoparticle contact area with the substrate with radius $a = (2R_1h-h^2)^{1/2}$ and the surface energy of the side area of the cap with height h. Evaluation of contribution of the van der Waals interactions of the deformed nanoparticle of average density ρ_p with a substrate requires integration of the long-range van der Walls potential[5] of magnitude ε_w over the particle height

$$U_{vdw}(h) \approx -\varepsilon_w\rho_p\sigma^3\pi\int_0^h \frac{\rho^2(z)}{(z+d_0)^3}\,dz$$

$$= -\varepsilon_w\rho_p\sigma^3\pi\int_0^h \frac{(h-z)(2R_1-h+z)}{(z+d_0)^3}\,dz \tag{A.3}$$

where $\rho(z)$ is the radius of the spherical cap at the distance z from the adsorbing surface, d_0 is the distance of the closest approach. Performing integration we arrive at

$$U_{vdw}(h) \approx -\varepsilon_w\rho_p\sigma^3\pi[\frac{(2R_1-h)h^2(h+2d_0)}{2d_0{}^2(h+d_0)^2}+\frac{(h-R_1)h^2}{(h+d_0)^2d_0}$$

$$-\log\left(\frac{h}{d_0}+1\right)-\frac{(4h+3d_0)d_0}{2(h+d_0)^2}+\frac{3}{2}] \tag{A.4}$$

For the systems with only van der Waals interactions one can relate the surface and interfacial energies to the system density and strength of the van der Waals interactions. In this case surface energy of the polymer−substrate interface γ_{ps} is equal to

$$\gamma_{ps} = \gamma_p+\gamma_s-\frac{\varepsilon_w\rho_p\sigma^2}{2d_0{}^2} \tag{A.5}$$

where γ_p is the polymer surface energy and γ_s is the substrate surface energy. Using eq A.5 we can relate the parameters of the

van der Waals interactions with the work of adhesion[5]

$$W = \gamma_p + \gamma_s - \gamma_{ps} = \frac{\varepsilon_w \rho_p \sigma^2}{2{d_0}^2} \quad (A.6)$$

The final contribution to the nanoparticle free energy is due to elastic energy of the particle deformation. Unfortunately, even with the simplifying assumptions of a spherical cap deformation, a rigorous computation of the displacement field for such deformation is a difficult task. Thus, we will apply a simplified approach developed in ref 16 to obtain the stress and the displacement fields in the deformed nanoparticle. The stress exerted by a deformed nanoparticle on the surface of semi-infinite half space is

$$\sigma(\rho) = \tilde{\sigma}_0(1-\rho^2/a^2)^{-1/2} + \tilde{\sigma}_1(1-\rho^2/a^2)^{1/2} \quad (A.7)$$

The displacement field of the nanoparticle which generate this stress is equal to

$$u_z(\rho) = \frac{\pi a}{K}\left(\tilde{\sigma}_0 + \frac{\tilde{\sigma}_1}{2}\left(1-\frac{\rho^2}{2a^2}\right)\right) \quad (A.8)$$

where $\tilde{\sigma}_0 = K(\Delta h/a - a/R_p)/\pi$, $\tilde{\sigma}_1 = K(2a/R_p)/\pi$, and $K = 2G/(1-\nu)$ is the nanoparticle rigidity. Taking this into account the elastic energy of the nanoparticle is estimated as follows

$$U_{el}(h) = \frac{1}{2}\int d^2\mathbf{x} u_z(\mathbf{x})\sigma(\mathbf{x}) = K\left[\Delta h^2 a - \frac{2}{3}\frac{\Delta h a^3}{R_p} + \frac{1}{5}\frac{a^5}{{R_p}^2}\right] \quad (A.9)$$

The equilibrium nanoparticle height is obtained from minimization of the total particle free energy

$$F(h) = U_s(h) + U_{vdw}(h) + U_{el}(h) \quad (A.10)$$

with respect to the nanoparticle height h. The scaling analysis of the nanoparticle deformation can be performed in the limit of small particle deformations for which $\Delta h/R_p \ll 1$. In this limit the nanoparticle free energy reduces to

$$F(\Delta h) \propto -2\pi W R_p \Delta h + \pi\gamma_p \Delta h^2 + \frac{7\sqrt{2}}{15} K {R_p}^{1/2} \Delta h^{5/2} \quad (A.11)$$

Appendix B: Simulation Details

We have performed molecular dynamics simulations of the adhesion of a spherical nanoparticle to a substrate. The nanoparticle was made of N_{ch}-chains with the degree of polymerization $N = 32$. The chains were cross-linked at different cross-linking densities in order to control the nanoparticle elastic modulus. In our coarse-grained molecular dynamics simulations the interactions between monomers forming a nanoparticle were modeled by the truncated-shifted Lennard-Jones (LJ) potential[19]

$$U_{LJ}(r_{ij}) = \begin{cases} 4\varepsilon_{LJ}\left[\left(\frac{\sigma}{r_{ij}}\right)^{12} - \left(\frac{\sigma}{r_{ij}}\right)^{6} - \left(\frac{\sigma}{r_{cut}}\right)^{12} + \left(\frac{\sigma}{r_{cut}}\right)^{6}\right] & r \le r_{cut} \\ 0 & r > r_{cut} \end{cases} \quad (B.1)$$

where r_{ij} is the distance between ith and jth beads and σ is the bead (monomer) diameter. The cutoff distance for the polymer−polymer interactions was set to $r_{cut} = 2.5\sigma$ and the value of the Lennard-Jones interaction parameter was equal to 1.5 k_BT. This choice of parameters corresponds to poor solvent conditions for the polymer chains.

The connectivity of the beads into polymer chains and the cross-link bonds were maintained by the finite extension nonlinear elastic (FENE) potential

$$U_{FENE}(r) = -\frac{1}{2}k_{spring}{R_{max}}^2 \ln\left(1-\frac{r^2}{{R_{max}}^2}\right) \quad (B.2)$$

with the spring constant $k_{spring} = 30k_BT/\sigma^2$ and the maximum bond length $R_{max} = 1.5\sigma$. The repulsive part of the bond potential is given by the truncated-shifted LJ potential with $r_{cut} = (2)^{1/6}\sigma$ and $\varepsilon_{LJ} = k_BT$. In our simulations we have excluded 1−2 LJ-interactions such that monomers connected by a bond only interacted through the bonded potential.

The presence of the substrate was modeled by the external potential

$$U(z) = \varepsilon_w\left[\frac{2}{15}\left(\frac{\sigma}{z}\right)^9 - \left(\frac{\sigma}{z}\right)^3\right] \quad (B.3)$$

where ε_w was equal to 1.5 k_BT, 2.25 k_BT, and 3.0 k_BT. The long-range attractive part of the potential z^{-3} represents the effect of van der Waals interactions generated by the substrate half-space. The system was periodic in x and y directions with dimensions $L_x = L_y = L_z = 4R_0$ where R_0 is the radius of a cavity for nanoparticle preparation (see discussion below).

Simulations were carried out in a constant number of particles and temperature ensemble. The constant temperature was maintained by coupling the system to a Langevin thermostat implemented in LAMMPS.[19] In this case, the equation of motion of the ith particle with mass m is

$$m\frac{d\vec{v}_i(t)}{dt} = \vec{F}_i(t) - \xi\vec{v}_i(t) + \vec{F}_i^R(t) \quad (B.4)$$

where $\vec{v}_i(t)$ is the ith bead velocity and $\vec{F}_i(t)$ is the net deterministic force acting on ith bead. $\vec{F}_i^R(t)$ is the stochastic force with zero average value $\langle\vec{F}_i^R(t)\rangle = 0$ and δ-functional correlations $\langle\vec{F}_i^R(t)\vec{F}_i^R(t')\rangle = 6\xi k_BT\delta(t-t')$. The friction coefficient ξ was set to $\xi = m/\tau_{LJ}$, where τ_{LJ} is the standard LJ-time $\tau_{LJ} = \sigma(m/\varepsilon_{LJ})^{1/2}$. The velocity-Verlet algorithm with a time step $\Delta t = 0.01\tau_{LJ}$ was used for integration of the equations of motion (eq B.4). All simulations were performed using LAMMPS.[19]

The simulations began with creating cross-linked nanoparticles. To create a nanoparticle we first placed N_{ch} noninteracting chains inside a cavity with radius R_0 made of bead-like overlapping particles with diameter σ. The radius of the spherical cavity, R_0, and the system sizes are listed in Table 1.

The interaction between beads forming a cavity and polymers was pure repulsive with $r_{cut} = (2)^{1/6}\sigma$ and $\varepsilon_{LJ} = k_BT$. During the initial simulation run lasting $t = 10^4\,\tau_{LJ}$ we set the diameter of the bead for polymer−polymer interactions to zero such that chains could easily pass through each other and equilibrate their conformations. This followed by the simulation run with duration $t = 10^4\,\tau_{LJ}$ during which we increased the bead diameter for polymer−polymer interactions from zero to σ. After the growth of the beads was completed the system was equilibrated for additional $t = 10^4\,\tau_{LJ}$ (see Figure 5a).

The next step involved cross-linking of polymer chains within a cavity. During this procedure neighboring monomers were randomly cross-linked by the FENE bonds if they are within 1.5 σ cutoff distance from each other. One cross-link bond was allowed per each monomer, thus creating a randomly cross-linked network. The elastic properties of the network were varied by changing the number of cross-links per particle. After completion of the

(19) Plimpton, S. *J. Comput. Phys.* **1995**, *117*(1), 1–19.

Table 1. System Sizes and Nanoparticle Parameters

R_0 [σ]	N_{ch}	R_p [σ]	$\rho_p\sigma^3$	$\rho_c\sigma^3$	G [k_BT/σ^3]	R_0 [σ]	N_{ch}	R_p [σ]	$\rho_p\sigma^3$	$\rho_c\sigma^3$	G [k_BT/σ^3]
11.304	161	10.904	0.968	0.043	0.023	26.740	2127	25.687	0.963	0.042	0.023
11.304	161	10.847	0.980	0.115	0.096	26.740	2127	25.588	0.973	0.114	0.096
11.304	161	10.802	0.990	0.189	0.214	26.740	2127	25.494	0.983	0.188	0.212
11.304	161	10.758	1.002	0.265	0.379	26.740	2127	25.397	0.994	0.263	0.375
11.304	161	10.714	1.014	0.342	0.597	26.740	2127	25.304	1.005	0.340	0.589
11.304	161	10.670	1.023	0.421	0.864	26.740	2127	25.213	1.016	0.418	0.855
16.400	491	15.775	0.966	0.043	0.023	31.836	3590	30.579	0.962	0.042	0.023
16.400	491	15.710	0.976	0.115	0.096	31.836	3590	30.465	0.972	0.114	0.096
16.400	491	15.644	0.987	0.189	0.213	31.836	3590	30.349	0.984	0.188	0.212
16.400	491	15.585	0.998	0.264	0.378	31.836	3590	30.237	0.994	0.263	0.376
16.400	491	15.522	1.009	0.341	0.593	31.836	3590	30.131	1.004	0.340	0.588
16.400	491	15.464	1.019	0.420	0.860	31.836	3590	30.020	1.015	0.418	0.855
20.536	964	19.737	0.964	0.042	0.023	35.973	5179	34.549	0.962	0.042	0.023
20.536	964	19.659	0.975	0.115	0.096	35.973	5179	34.420	0.972	0.114	0.096
20.536	964	19.582	0.986	0.188	0.213	35.973	5179	34.293	0.983	0.188	0.212
20.536	964	19.508	0.996	0.264	0.377	35.973	5179	34.171	0.993	0.263	0.375
20.536	964	19.437	1.007	0.341	0.591	35.973	5179	34.047	1.004	0.340	0.588
20.536	964	19.367	1.016	0.418	0.855	35.973	5179	33.925	1.014	0.418	0.853

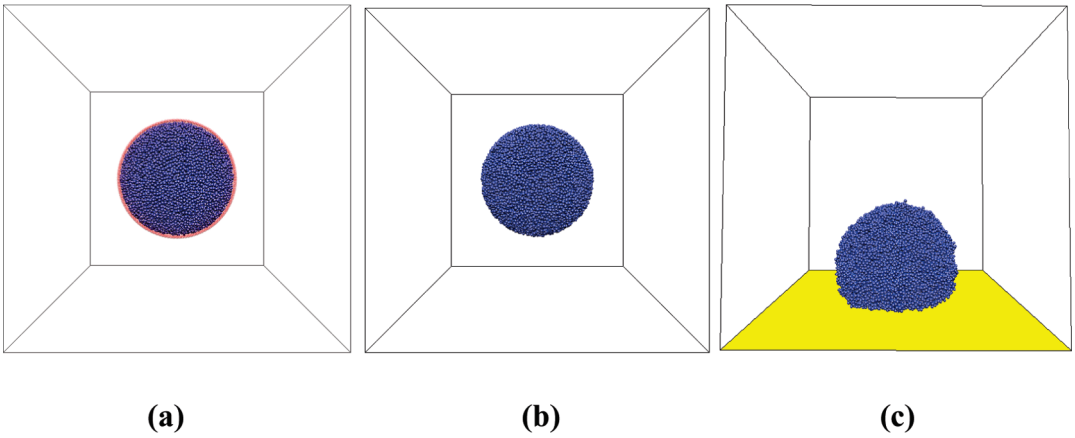

Figure 5. Snapshots of the simulation box during (a) equilibration of chains inside a cavity, (b) relaxation of cross-linked nanoparticle, and (c) adhesion of nanoparticle to a substrate.

cross-linking process the confining cavity was removed and a system was relaxed by performing NVT molecular dynamics simulation run lasting 10^4 τ_{LJ}. This completed the nanoparticle preparation procedure (see Figure 5b). The nanoparticle size R_p was obtained from the mean-square average value of the particle radius of gyration, $R_p = (5\langle R_g^2\rangle/3)^{1/2}$. The equilibrium nanoparticle sizes, average monomer and cross-linking densities are summarized in Table 1.

Modeling of the nanoparticle adhesion to the substrate was initiated with placement of the nanoparticle center of mass at distance $z = R_0 + \sigma$ from the substrate. After that the system was equilibrated for $t = 2 \times 10^4$ τ_{LJ} and the final 10^4 τ_{LJ} were used for the data collection. Figure 5c shows the snapshot of the adsorbed nanoparticle at the substrate.

The values of the nanoparticle shear modulus were obtained by using interpolation expression for G as a function of the cross-linking density[18]

$$\frac{G\sigma^3}{k_BT} = a(\rho_c\sigma^3)^2 + b\rho_c\sigma^3 \qquad \text{(B.5)}$$

with the numerical coefficients $a = 3.98$ and $b = 0.38$.

A surface energy of a nanoparticle interface was evaluated by performing molecular dynamics simulations of the 3-D periodic system of a slab of a polymeric network with the same set of the LJ-interaction and bond parameters, monomer and cross-linking density as our nanoparticles. For these simulations the box size was 14.537 $\sigma \times$ 14.537 $\sigma \times$ 29.074σ and the total number of monomers was equal to 3072 (96 chains with the degree of polymerization 32). The simulation runs continued for 2×10^4 τ_{LJ} with the last 10^4 τ_{LJ} used for the data analysis. The surface energy then was obtained by integrating the difference of the normal $P_N(z)$ and tangential $P_T(z)$ to the interface components of the pressure tensor across the interface. Note, that in our

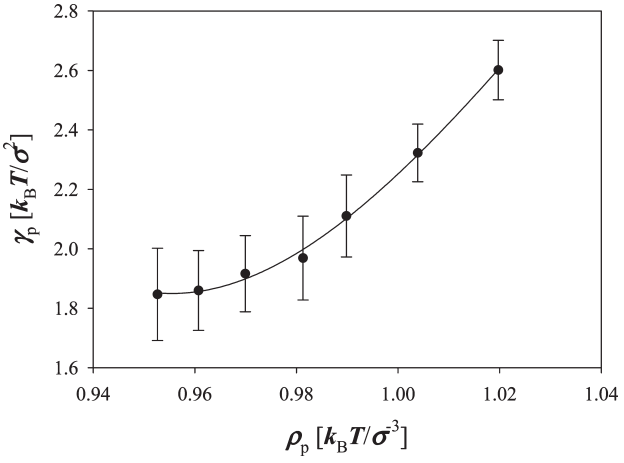

Figure 6. Dependence of the polymer surface energy on polymer density. The line is given by the equation $y = 1128.5 - 3299.5x + 3204.42\,x^2 - 1031.1\,x^3$.

simulations the z direction was normal to the interface.

$$\gamma = \int_{-\xi}^{\xi} (P_N(z) - P_T(z))\ \mathrm{d}z \qquad \text{(B.6)}$$

where 2ξ is the thickness of the interface that was determined from the monomer density profile as an interval within which the monomer density changes from zero to the bulk value. Figure 6 show dependence of the surface energy as a function of the polymer density. Note that a cross-linking density is related to polymer density (see Table 1). The surface energy increases with increasing the number of cross-links. This is due to increase of the average monomer density with increasing the cross-linking density.